

Simple Synthesis of Vanadium Oxide (V_2O_5) Nanorods in Presence of CTAB Surfactant

Majid Farahmandjou, Nilofar Abaeian

Department of Physics, Varamin Pishva Branch, Islamis Azad University, Varamin, Iran

Email address:

farahmandjou@iauvaramin.ac.ir (M. Farahmandjou)

To cite this article:

Majid Farahmandjou, Nilofar Abaeian. Simple Synthesis of Vanadium Oxide (V_2O_5) Nanorods in Presence of CTAB Surfactant. *Colloid and Surface Science*. Vol. 1, No. 1, 2016, pp. 10-13. doi: 10.11648/j.css.20160101.13

Received: November 25, 2016; **Accepted:** December 8, 2016; **Published:** January 16, 2017

Abstract: Structural and morphological properties of vanadium oxides (V_2O_5) nanoparticles have been studied. V_2O_5 nanoparticles were synthesized using a simple chemical method by sodium metavanadate as precursor and Cetyltrimethylammonium bromide (CTAB) as surfactant. The samples were characterized by high resolution transmission electron microscopy (HRTEM), field effect scanning electron microscopy (FESEM) and X-ray diffraction (XRD). As there are many forms of vanadium oxides produced during this process, x-ray diffraction (XRD) technique was used to identify V_2O_5 phase. The size of as-prepared nanoparticles was around 5 nm as estimated by HRTEM technique and average diameter of annealed one was around 9 nm. The surface morphological studies from SEM depicted the formation of nanorods after annealing process. The effect of CTAB surfactant on the particle morphology was also studied and the results show that the size of particles reduce to 10 nm in presence of CTAB surfactant. FTIR spectrum shows the presence of V-O and V-O-V stretching mode of V_2O_5 . The UV-vis absorption show the small band gap is found to be 2.20 eV.

Keywords: Vanadium Oxide Nanoparticles, CTAB, Surfactant, Chemical Synthesis

1. Introduction

Nanotechnology has large potential benefits to a range of areas. Nanomaterials have the potential to improve the environment through the development of new solutions to environmental problems. Nanotechniques have been touted as a new technology that may surpass the physical and chemical limitations of materials made from microparticles. Vanadium oxides constitute an important class of materials employed in different technological applications, and present a fascinating and broad range of chemical and physical properties resulting from the various metal oxidation states (from +II to +V) and the different V-O coordination geometries. Vanadium oxygen systems (V_2O_5 , VO_2) are prototype strongly-correlated materials that have been widely-studied by theoretical and experimental condensed-matter and materials community for more than half a century [1, 2]. Vanadium oxide is a well-known catalyst among various metal oxides [3], and so many fundamental studies have been developed wide-spreadingly centering around catalytic oxidation [4, 5]. They show metal-semiconductor transition, which implies an abrupt change in optical and

electrical properties [6]. That is why this oxide is used in thermal sensing and switching. Vanadium pentoxide based materials are known to display several types of chromogenic effects [7], as a window for solar cells [8] and for transmittance modulation in smart windows with potential applications in architecture, automobiles and nanomedicine [9]. It shows an atypical behavior because it cannot be defined exactly either as a cathodically or as anodically coloring material. V_2O_5 exhibit multi-colored electrochromism allowing the use in electrochromic displays color filters and other optical devices [1, 10]. Transition metal oxides have been a subject of research in recent years in view of their fundamental and technological aspects. Among these, vanadium creates many compounds with oxygen; these have different structural, optical and chemical properties. Meaningful differences between the properties of different phases of vanadium oxides like VO, VO_2 , V_2O_3 and V_2O_5 depend on their structure, which determines other properties [11, 12]. Different forms of vanadium oxides can be obtained by changing the deposition process parameters, or by post-process treatment, e.g., additional annealing [13]. From the application point of view, the most interesting vanadium oxides are VO_2 and V_2O_5 . Vanadium dioxide is a

very good candidate for thermochromic coatings due to the change of properties from semiconducting to semimetal at 68°C. Vanadium pentoxide (V_2O_5) is a thermodynamically stable form which exhibits electrochromic properties. V_2O_5 thin films can also be used in optical filters, reflectance mirrors, smart windows and surfaces with tunable emittance for temperature control of space vehicles [14]. It can be received by selecting deposition parameters or by the annealing of VO_2 above 350°C [15]. The main synthetic route to vanadiumoxides by wet chemical methods is the sol-gel process, generally starting from a vanadyl alkoxide, or from vanadates, vanadic acid or vanadium oxychloride. These commercial sol-gel precursors contain vanadium centres in the +V formal oxidation state, requiring chemical reduction steps for the preparation of the lower valence oxides. The sol-gel process provides oxides with different structures, morphologies, stoichiometries, crystallinity degrees and particle sizes when a suitable choice of precursor and synthetic conditions is made. In this article, vanadium oxide nanoparticles are fabricated by using sol-gel method. Structural and surface morphological properties are discussed by XRD, HRTEM, UV-vis and FESEM analyses.

2. Experimental Detail

Vanadium oxide nanoparticles were synthesized by a new synthesis according to the following manner. Firstly, 0.6 g sodium metavanadate was completely dissolved in 100 mL pure water with stirring at room temperature. Ammonium chloride (1 g) was then added to the solution until dissolved completely. The color of solution changed from muddy color to transparent color which after a few minutes changed to foggy color. After 5 min, 1 g, Cetyltrimethylammonium bromide (CTAB) was added to the solution and synthesis temperature was increased to 85°C. The color of solution changed from orange color to dark brown color. The pH was between 6 and 7 during the synthesis. After one hour, the color of solution changed to transparent yellow color. The product was evaporated for 2 hours, cooled to room

temperature and finally calcined at 600°C for 4 hours. All analyses were done for samples without any washing and more purification. The specification of the size, structure and optical properties of the as-synthesis and annealed vanadium oxide nanoparticles were carried out. X-ray diffractometer (XRD) was used to identify the crystalline phase and to estimate the crystalline size. The XRD patterns were recorded with 2θ in the range of 4-85° with type X-Pert Pro MPD, Cu- K_{α} ; $\lambda = 1.54 \text{ \AA}$. The morphology was characterized by field emission scanning electron microscopy (SEM) with type KYKY-EM3200, 25 kV and transmission electron microscopy (TEM) with type Zeiss EM-900, 80 kV. All the measurements were carried out at room temperature.

3. Result and Discussion

X-ray diffraction (XRD) at 40 kV was used to identify crystalline phases and to estimate the crystalline sizes. Figure 1(a) shows the XRD pattern of aluminium oxide before annealing. Figure 1(b) shows the X-ray diffraction patterns of the powder after heat treatment at 600°C for 4 hours. The XRD patterns showed this sample has sharp peaks 2θ angle at the peak position at 25.2°, 32°, 33.5°, 37.5°, 45° and 51° with (101), (400), (011), (301), (411) and (002) diffraction planes, respectively are in accordance with the rhombohedral structure of the V_2O_5 phase. The mean size of the ordered V_2O_5 nanoparticles has been estimated from full width at half maximum (FWHM) and Debye-Scherrer formula according to the following:

$$D = \frac{0.89\lambda}{B \cos \theta} \quad (1)$$

where, 0.89 is the shape factor, λ is the x-ray wavelength, B is the line broadening at half the maximum intensity (FWHM) in radians, and θ is the Bragg angle. The mean size of annealed V_2O_5 nanoparticles was around 9 nm from this Debye-Scherrer equation.

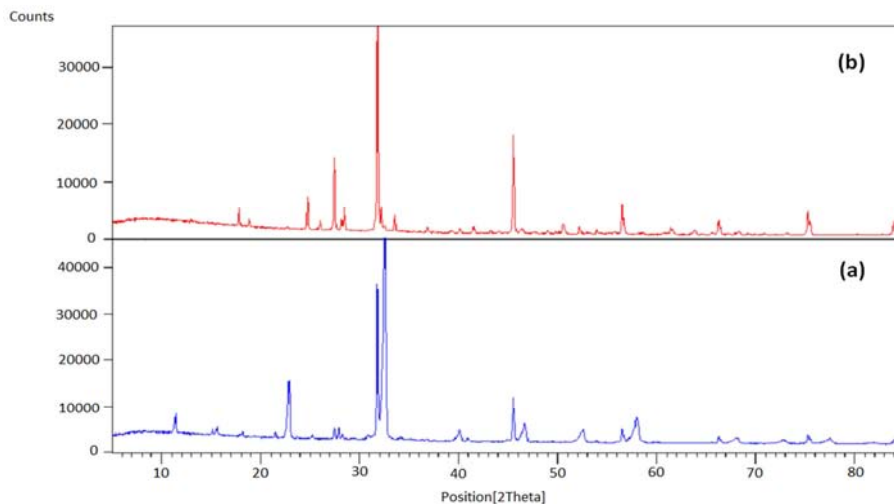


Figure 1. XRD patterns of (a) as-synthesized and (b) annealed V_2O_5 nanoparticles at 600°C.

SEM analysis was used for the morphological study of nanoparticles of V_2O_5 samples. These analyses show that the nanoparticles are appeared in the samples by increasing annealing temperature. Figure 2(a) shows the SEM image of the as-prepared V_2O_5 grains with formation of clusters. Figure 2(b) shows the SEM image of the annealed V_2O_5 nanorod at 600°C for 4 hours. The smallest diameter of V_2O_5 samples formed was about 9 nm.

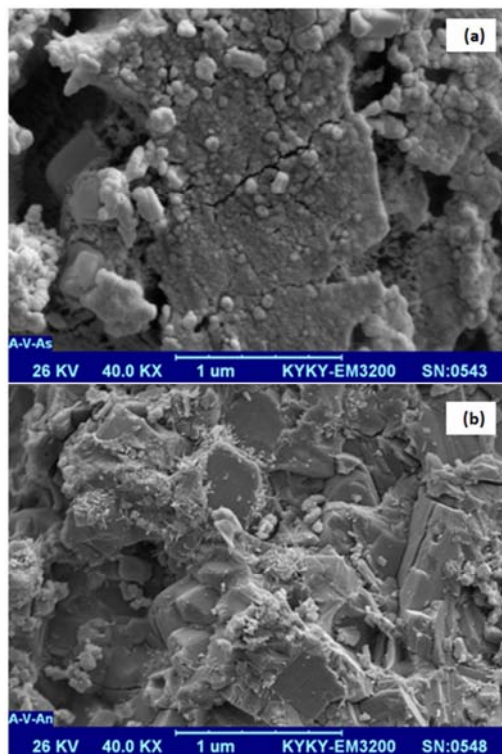


Figure 2. SEM images of the (a) as-prepared (b) annealed V_2O_5 nanorods at 600°C .

Average particle size of the as-prepared powders was measured by using high resolution TEM. The transmission electron microscopic analysis was carried out to confirm their

growth pattern and the distribution of the crystallites. TEM analysis was carried out to confirm the actual size of the particles, their growth pattern and the distribution of the crystallites. Figure 3 shows the as-synthesized TEM image of V_2O_5 nanoparticles prepared by sol-gel route. The uniform structure of the vanadium oxide was formed with size of about 5 nm.

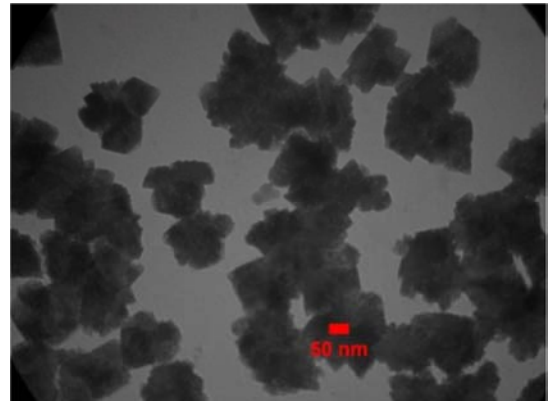


Figure 3. TEM image of the as-prepared V_2O_5 sample.

According to figure 4, the infrared spectrum (FTIR) of the synthesized V_2O_5 nanoparticles was in the range of $400\text{--}4000\text{ cm}^{-1}$ wave-number which identifies the chemical bonds as well as functional groups in the compound. The large broad band at 3135 cm^{-1} and 3037 cm^{-1} are ascribed to the O-H and C-H groups. The absorption picks around 1401 cm^{-1} is due to the bending vibration of C=C vibration. FTIR spectra of V_2O_5 nanoparticles exhibited three characteristic vibration modes: V=O vibrations at 967 cm^{-1} , the V-O-V symmetric stretch around 531 cm^{-1} and the V-O-V asymmetric stretch at 730 cm^{-1} . As clearly seen, the bands appearing, between 950 cm^{-1} and 1020 cm^{-1} were assigned to a stretching mode (δ V-O). Bands between 700 cm^{-1} and 900 cm^{-1} were ascribed to the bridging V-O-V stretching.

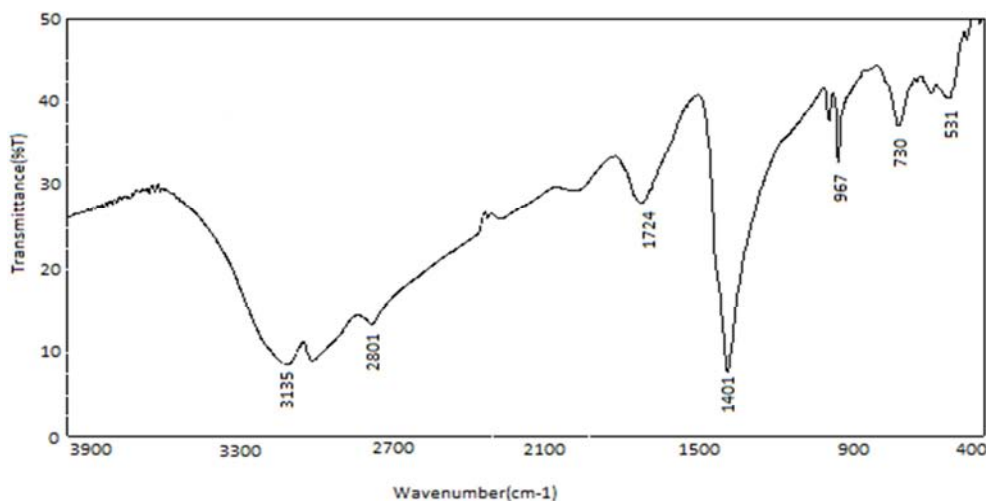


Figure 4. FTIR spectrum of V_2O_5 sample.

UV-visible absorption spectral study may be assisted in understanding electronic structure of the optical band gap of the material. Absorption in the near ultraviolet region arises from electronic transitions associated within the sample. UV-Vis absorption spectra of as-prepared and annealed V_2O_5 are shown in Figure 5. For as-synthesized V_2O_5 nanoparticles (Figure 5(a)), the strong absorption band at low wavelength near 545 nm correspond to band-gap energy of 2.20 eV and for annealed V_2O_5 at 1000°C (Figure 5(b)), the strong absorption band at low wavelength near 550 nm correspond to 2.26 eV. The band/peak in the spectrum located at around 400-700 nm are observed to be shifted towards lower wavelength side, which clearly shows the blue shift. It indicates the absorption positions depend on the morphologies and sizes of V_2O_5 . The UV absorption ability of V_2O_5 is related with band gap energy.

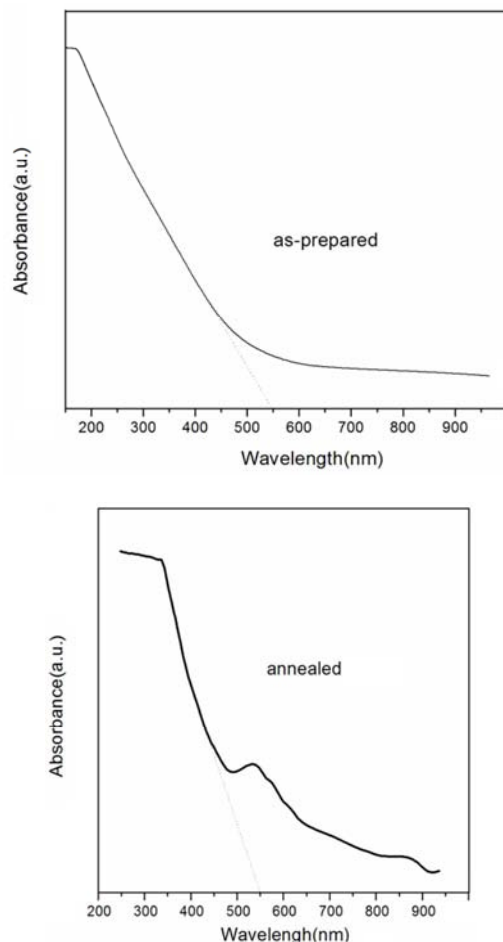


Figure 5. UV-vis absorption spectra of V_2O_5 nanoparticles: (a) as-synthesized (b) annealed sample.

4. Conclusion

Novel vanadium oxide nanorods were successfully prepared using sodium metavanadate as precursor and CTAB

as surfactant. XRD spectrum shows rhombohedral structure of V_2O_5 annealed at 600°C. From SEM images, it is clear that with increasing temperature the morphology of the particles changes to nanorod shaped and the size of particles decreases to 9 nm. TEM image exhibits that the uniform as-synthesized V_2O_5 nanoparticles prepared by sol-gel route with an average diameter about 5 nm. Finally FTIR spectrum shows the presence of V-O and V-O-V stretching mode of V_2O_5 . The UV-vis absorption show the small band gap is found to be 2.20 eV.

Acknowledgments

The authors are thankful for the financial support of varamin pishva branch at Islamic Azad University for analysis and the discussions on the results.

References

- [1] S. F. Cogan, N. M. Nguyen, S. T. Perrotti, R. D. Rauh, *Proc. Soc. Photo-Opt. Instrum. Eng.* 57, 1016 (1988).
- [2] C. G. Granqvist, *Solid State Ionics* 70, 678 (1994).
- [3] C. M. Julien, *Ionics* 2, 169 (1996).
- [4] M. E. Spahr, P. S. Bitterli, R. Nesper, O. Haas, P. Novak, *J. Electrochem. Soc.* 146, 2780 (1999).
- [5] E. A. Meulenkamp, W. van Klinken, A. R. Schlatmann, *Solid State Ionics* 126, 235 (1999).
- [6] J. Haber, M. Witko, R. Tokarz, *Appl. Catalysis A General* 157, 3 (1997).
- [7] C. M. Lampert, C. G. Granqvist, editors, *Large Area Chromogenic materials and Devices for Transmittance Control*, Bellingham: SPIE, (1990).
- [8] S. D. Hansen, C. R. Aita, *J. Vac. Sci. Technol.* A3, 660 (1985).
- [9] MSR. Khan, K. A. Khan, W. Estrada, C. G. Granqvist, *J. Appl. Phys.* 5, 69(1991).
- [10] Y. Fujita, K. Miyazaki, T. Tatsuyama, *Jap. J. Appl. Phys.* 24, 1082 (1985).
- [11] K. Sieradzka, D. Wojcieszak, D. Kaczmarek, J. Domaradzki, G. Kiriakidis, E. Aperathitis, V. Kambalafka, F. Placido, S. Song, *Optica Applicata*, (2011), 9 463-469.
- [12] V. S. Reddy Channu, R. Holze, B. Rambabu, *Soft Nanoscience Letters*, (2011), 1, 66-70.
- [13] M. Mousavi, A. Kompany, N. Shahtahmasebi, M. M. Bagheri-Mohagheghi, *Adv. Manuf.* (2013), 1, 320-328.
- [14] B. Vijaykumar, K. Sangshetty, G. Sharanappa, *Int. J. Eng. Res. App.* (2012) 2, 611-616.
- [15] N. N. Dinh, T. T. Thao, V. N. Thuc, N. T. Thuy, *J. Sci. Math. Phys.*, (2010), 26 201-206.